DESIGN OF AXIALLY-SYMMETRIC CASSEGRAIN AND GREGORIAN CONFIGURATIONS WITH REDUCED SPILLOVERS

Fernando J. S. Moreira* and Aluizio Prata, Jr.
University of Southern California
Los Angeles, CA 90089-0271

A. Introduction

One of the tasks faced by antenna designers is the accomplishment of radiation patterns satisfying restrict specifications. Generally, low sidelobe levels are required in conjunction with low spillover losses. In a dual-reflector configuration, these losses are mainly related to the feed radiation past the subreflector (forward spillover) and the subreflector radiation past the main reflector (backward spillover). The backward spillover can be reduced by increasing the roll-off of the subreflector radiation, which is controlled by the shape of the subreflector and the associated feed illumination. The forward spillover may then be reduced by a convenient metallic shield placed around the subreflector rim. However, the metallic shield can be understood as an extention of the subreflector, arising the possibility of shaping the whole structure (subreflector/shield) as a single one with a relatively larger feed taper, simultaneously obtaining reduced forward and backward spillovers. Aiming this objective, the present work discusses a simple formulation, based on the Uniform Theory of Diffraction (UTD) [1], relating the subreflector-edge-directed feed illumination (desirably low enough to reduce the forward spillover) with the associated aperture-rim electric field (prescribed for the antenna shaping), while naturally providing a large subreflector-radiation roll-off. Although only axially-symmetric dual-reflector Cassegrain and Gregorian systems are considered in this work, the basic principles may be extended to more complex geometries.

B. Subreflector Roll-Off Basic Formulation

Aiming the control of the subreflector roll-off and the backward spillover, an analytical study of the field behavior around the subreflector reflection boundary is conducted, based on the UTD [1]. The electric field is then expressed as

$$\vec{E}_T(R_B, \theta_B \approx 0) \approx \vec{E}_{GO}(R_B, \theta_B \approx 0) + \vec{E}_D(R_B, \theta_B \approx 0) , \qquad (1)$$

where, with the help of Figs. 1 and 2, R_B and θ_B locate the observation point in the plane of incidence (noticing that $\theta_B < 0$ inside the reflection region) and $\vec{E}_{GO}$ and $\vec{E}_D$ are the Geometrical Optics (GO) and diffraction components of the electric field, respectively. Around the reflection boundary, these components are strongly related with the scattering mechanisms associated with the subreflector edge-point B.

The subreflector roll-off is obviously related with $\partial E_T/\partial\theta_B$. This derivative is simply obtained by noticing that, for a circularly-symmetric feed illumination upon an axially-symmetric subreflector and around the reflection boundary ($\theta_B \approx 0$), the electric-field orientation does not significantly vary with the plane of incidence [2]. Thus, the problem at hand can be treated as a scalar one and

$$\frac{\partial}{\partial\theta_B} E_T(R_B, \theta_B \approx 0) \approx \frac{\partial}{\partial\theta_B} E_{GO}(R_B, \theta_B \approx 0) + \frac{\partial}{\partial\theta_B} E_D(R_B, \theta_B \approx 0) . \qquad (2)$$

The derivative of E_{GO} will be simply represented as

$$\frac{\partial}{\partial\theta_B} E_{GO}(R_B,\theta_B) = E_{GO}(R_B,\theta_B=0)\ D_{GO}(R_B,\theta_B) \left[\frac{1-Sign(\theta_B)}{2}\right], \quad (3)$$

where D_{GO} is assumed continuous across the reflection boundary and $Sign(\theta_B) = -1$ and $+1$ for $\theta_B \leq 0$ and $\theta_B > 0$, respectively. The derivative of the diffraction component can be shown equal to [1],[2]

$$\frac{\partial}{\partial\theta_B} E_D(R_B,\theta_B) \approx -E_{GO}(R_B,\theta_B=0)\left[\sqrt{\frac{j\,R_B\,\rho_{1r}^B/\lambda}{R_B+\rho_{1r}^B}} - \frac{R_B\ Sign(\theta_B)}{4\,(R_B+\rho_{2r}^B)\,\tan\theta_U}\right], \quad (4)$$

where θ_U is the negative angle between the reflection boundary and the symmetry axis (see Figs. 1 and 2) and ρ_{1r}^B and ρ_{2r}^B are the reflected-wavefront principal radii of curvature in the incidence and perpendicular planes, respectively.

From Eqs. 2–4 one readily observes a discontinuity in the electric-field derivative at the reflection boundary. This comes with no surprise, as the UTD ensures only the field continuity across the boundary [1]. To overcome this difficulty while achieving a simple and useful equation for the roll-off control, the above partial derivative (close to the reflection boundary) is approximated as the geometric average of Eq. 2 at both sides of the boundary, yielding (as $|E_T| \approx |E_{GO}|/2$ when $\theta_B \to 0^-$) [2]

$$\frac{\partial}{\partial\theta_B}|E_T(R_B,\theta_B\approx 0)| \approx |E_T(R_B,\theta_B\approx 0)|\left[D_{GO}(R_B,\theta_B) - \sqrt{\left|\frac{2\,R_B\,\rho_{1r}^B/\lambda}{R_B+\rho_{1r}^B}\right|}\,\right]. \quad (5)$$

C. Achievement of Reduced Forward and Backward Spillovers

The subreflector roll-off can be controlled by ρ_{1r}^B with the help of Eq. 5. Assuming that a uniform-phase aperture distribution is specified (maximum gain), ρ_{1r}^B can be obtained from the relation between the feed and antenna GO aperture fields [1]:

$$\left|\vec{E}_A^{GO}(\rho_A = D_M/2)\right| = \left|\vec{E}_F(B^-)\right| \left|\sqrt{\rho_{1r}^B/(R_{BU}+\rho_{1r}^B)}\ \sqrt{\rho_{2r}^B/(R_{BU}+\rho_{2r}^B)}\right|, \quad (6)$$

where $\vec{E}_A^{GO}$ is the GO aperture electric field, ρ_A is the distance between the aperture point and the symmetry axis, D_M is the aperture diameter, $\vec{E}_F(B^-)$ is the feed electric field just before reaching point B, and R_{BU} is the distance between points B and U (see Figs. 1 and 2). From Eq. 5 and knowing that D_{GO} is well behaved, the achievement of a large subreflector roll-off can, in principle, be obtained in three distinct ways. The first one (noticing that Eq. 5 varies linearly with $|E_T|$) is to increase the feed illumination towards the subreflector edge, which results on an increased forward spillover. The second option is to make $\rho_{1r}^B \approx -R_{BU}$, in which case a caustic is present near point U and, consequently, the approximations used to derive the above formulation are not valid at this region. The third option is to make $|\rho_{1r}^B| \to \infty$, which corresponds to a reflected wavefront with negligible curvature in the plane of incidence (and around the reflection boundary). From Eq. 6, the last option is directly obtained when

$$\left|\vec{E}_A^{GO}(\rho_A = D_M/2)\right| \approx \left|\vec{E}_F(B^-)\right|\ \sqrt{|\rho_{2r}^B/(R_{BU}+\rho_{2r}^B)|}\,. \quad (7)$$

As the shaping of a dual-reflector antenna generally departs from established feed and aperture field distributions, Eq. 7 may be used to derive the necessary conditions to obtain a large subreflector roll-off (reduced backward spillover) together with a desirably low subreflector-edge-directed feed illumination (reduced forward spillover).

Finally, the use of Eq. 7 requires the values of R_{BU} and ρ^B_{2r}, which are not known prior to the reflector shaping. However, the simple inspection of Figs. 1 and 2 shows that both parameters can be easily estimated. For this task, generalized classical configurations (and their closed-form design equations) may be employed [2],[3], also yielding an optimized starting point for the shaping procedure.

D. Numerical Results

The present formulation was applied in the GO shaping of an axially-symmetric Cassegrain system, depicted in scale in Fig. 3. The design aimed the envelope requirements of the ITU Recommendations 465-5 and 580-5 for earth stations operating in satellite communications [4], with the maximum possible gain. The main- and subreflector diameters are 100λ and 15λ, respectively, with a subreflector clearance of 2.5λ. The antenna length is about 60λ. To enhance the front-to-back ratio of the antenna pattern, the main reflector is closed by extending the corresponding surface (dashed lines in Fig. 3). A corrugated horn with a flare semi-angle of 8° and an aperture diameter of 3λ was adopted. The feed gain is about 18 dBi with a high taper of 27.7 dB towards the subreflector-edge direction ($\theta = 35°$). With the above input parameters, a generalized classical configuration [3] was obtained to estimate the values of $R_{BU} \approx 44.2\lambda$ and $\rho^B_{2r} \approx 7.8\lambda$. These values, together with Eq. 7 and the known feed radiation, indicate that the GO aperture illumination (depicted in Fig. 4) at $\rho_A = 50\lambda$ should be about 15 dB below its maximum to accomplish a large subreflector roll-off (the final configuration has $\rho^B_{1r} \approx 275\lambda$). A complete presentation of the above design is conducted in Ref. [2].

A Moment-Method analysis (accounting for the feed structure and both reflectors) was performed to confirm the usefulness of the present formulation. Figures 5 and 6 show the radiation patterns of the feed/subreflector configuration and of the whole system, respectively, where $\theta = 0°$ corresponds to the feed boresight direction. From Fig. 5 one readily observes that a large subreflector roll-off was obtained ($\theta \approx 110°$). This large roll-off and the highly tapered feed radiation reduce the spillover losses and contribute to the accomplishment of sidelobe levels mainly below the ITU envelope (see Fig. 6). The present configuration has a gain (including the feed return loss) of 49.0 dBi, corresponding to an antenna efficiency of 80%.

References

[1] - R.G. Kouyoumjian and P.H. Pathak, "A Uniform Geometrical Theory of Diffraction for an Edge in a Perfectly Conducting Surface," Proc. IEEE, **62**, No. 11, pp. 1448–1461, Nov. 1974.

[2] - F.J.S. Moreira, "Design and Rigorous Analysis of Generalized Axially-Symmetric Dual-Reflector Antennas," Ph.D. dissertation, Univ. Southern California, Aug. 1997.

[3] - F.J.S. Moreira and A. Prata, Jr., "Generalized Classical Axially-Symmetric Dual-Reflector Antennas," 1997 IEEE AP-S International Symposium, Montreal, Canada, pp. 1402–1405, July 1997.

[4] - International Telecommunication Union—Radiocommunication (ITU-R), *S Series Recommendations - Fixed Satellite Service.*

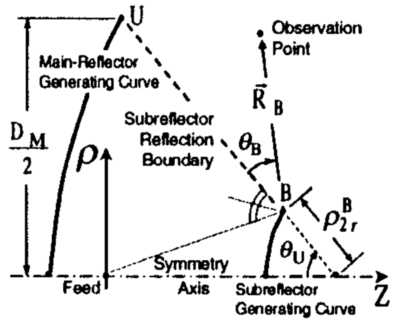

Fig. 1: Cassegrain Configuration.

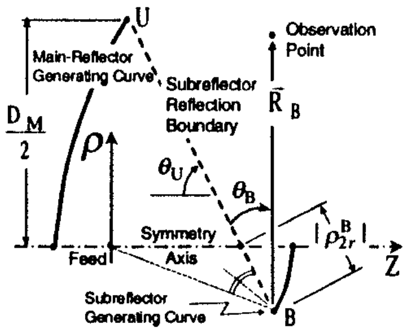

Fig. 2: Gregorian Configuration.

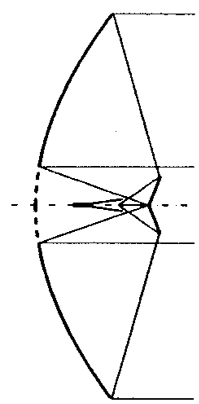

Fig. 3: Shaped Cassegrain Geometry.

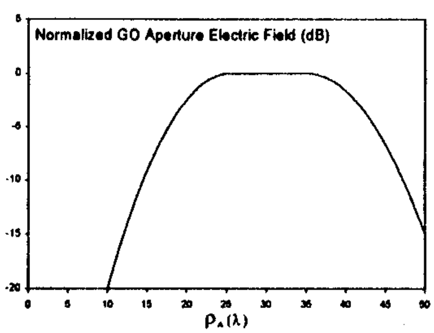

Fig. 4: Normalized GO Aperture Field.

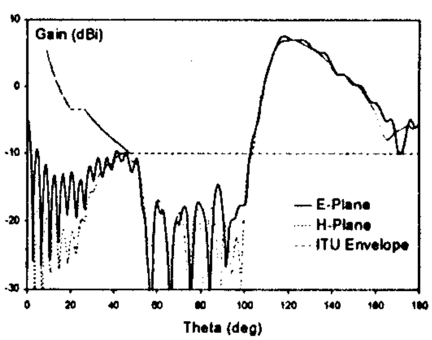

Fig. 5: Feed/Subreflector Pattern.

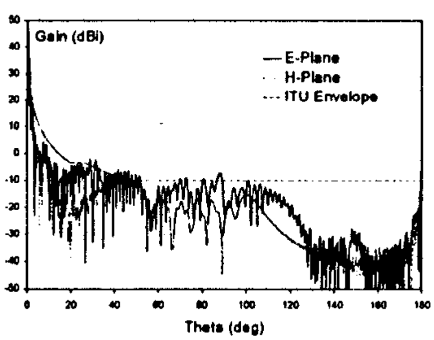

Fig. 6: Shaped Cassegrain Pattern.